

Calculation of the strain state under multipass wire drawing

Cite as: AIP Conference Proceedings **1785**, 040032 (2016); <https://doi.org/10.1063/1.4967089>
Published Online: 18 November 2016

Yu. N. Loginov, N. A. Babailov, and A. E. Pervukhin



View Online



Export Citation

ARTICLES YOU MAY BE INTERESTED IN

Deformation Analysis of Surface Defects in Wire Drawing

AIP Conference Proceedings **712**, 594 (2004); <https://doi.org/10.1063/1.1766591>

Evolution of surface defects in platinum alloy wire under drawing

AIP Conference Proceedings **1915**, 040032 (2017); <https://doi.org/10.1063/1.5017380>

Industrial recycling of technogenic wastes and mineral ore processing

AIP Conference Proceedings **1785**, 040046 (2016); <https://doi.org/10.1063/1.4967103>

AIP | Conference Proceedings

Get **30% off** all
print proceedings!

Enter Promotion Code **PDF30** at checkout



Calculation of the Strain State under Multipass Wire Drawing

Yu.N. Loginov^{1, a)}, N.A. Babailov^{2, b)} and A.E. Pervukhin^{1, a)}

¹ Ural Federal University, Ekaterinburg, Russian Federation.

² Institute of Engineering Science, UB RAS, Ekaterinburg, Russian Federation.

^{a)}Corresponding author: j.n.loginov@urfu.ru

^{b)} babailov@imach.uran.ru

Abstract. The process of multi-pass wire drawing is considered. A mathematical model of the wire drawing process is developed with the use of the CAE package. Simulation results are presented for 4 passes of drawing. Strain state is defined for all the passes of wire drawing.

INTRODUCTION

The drawing process is generally a calibrating operation enabling the required accuracy of manufacturing semi-finished products and improved surface roughness to be achieved. At the same time, a drawing method is often multicycle under production conditions if the process aims at a significant change in the product cross section. The example of this is copper wire production in the cable industry. It is difficult to remove such negative phenomena as breakage under real industrial conditions. Breakage localization at a certain wire diameter is often treated as exhaust of plasticity resource when the critical strain level is exceeded. It is obvious that breakage in this case must localize in the subsequent deformation runs, however it does not.

1. EXPERIMENTAL PROCEDURE

Figure 1 (a) shows a graph of breakage frequency distribution in copper wire production for electrical engineering, 0.2 mm diameter wire is produced from 8 mm diameter rod. The graph shows that the breakage peak falls on the intermediate wire sizes rather than on the minimum values, and this is contradictory to the popular opinion.

This paper proposes a hypothesis that the existing theory of fracture can adequately describe phenomena only for low-textured materials. Copper may be among these materials, but only when hot-rolled [1]. It was demonstrated in [2, 3] that copper is an easily textured material. For example, the elastic modulus for copper single crystals may vary three times, that is, it is heavily dependent on crystallite orientation, which changes during drawing [4, 5]. Crystallite orientation is additionally affected by strain rate [6] and the content of copper oxide particles [7]. In turn, the stress-strain state affects texture reorientation during drawing. The question arises as to how much the stress and strain distribution pattern will change in the drawing route.

2. CALCULATION PROCEDURE

The problem of the determination of the stress-strain state is solved with the application of the RAPID-2D CAE program developed at the Ural Federal University to calculate plastic deformation of materials exhibiting strain and strain-rate hardening.

The initial data for calculation are as follows: die angle $\alpha = 10^\circ$. The following actual wire drawing sequence (or die diameters) of a copper wire production facility is used:

8.00 mm \rightarrow 6.53 mm \rightarrow 5.37 mm \rightarrow 4.48 mm \rightarrow 3.76 mm.

In accordance with the wire drawing sequence, the current extension ratio is calculated as $\lambda_i = d_{i-1}^2 / d_i^2$, where d_i is the current wire diameter in the i -th pass. The accumulated extension ratio is simultaneously calculated by the formula $\lambda_{\Sigma i} = \prod \lambda_i$, the accumulated relative reduction in the drawing pass being calculated as

$$\varepsilon_{\Sigma i} = 100 * \frac{\lambda_{\Sigma i} - 1}{\lambda_{\Sigma i}}. \quad (1)$$

At a strain rate of 50 s^{-1} , which corresponds within the order of magnitude to the commercial operating speed of a drawing machine, the hardening curve for oxygen containing copper is described by the following equation:

$$\sigma_s = 80 + 283\varepsilon^{0.018} \quad (2)$$

To estimate the intensity of copper hardening, the stress derivative with respect to the amount of strain is used,

$$\frac{d\sigma_s}{d\varepsilon} = 33.39 * \varepsilon^{-0.882}. \quad (3)$$

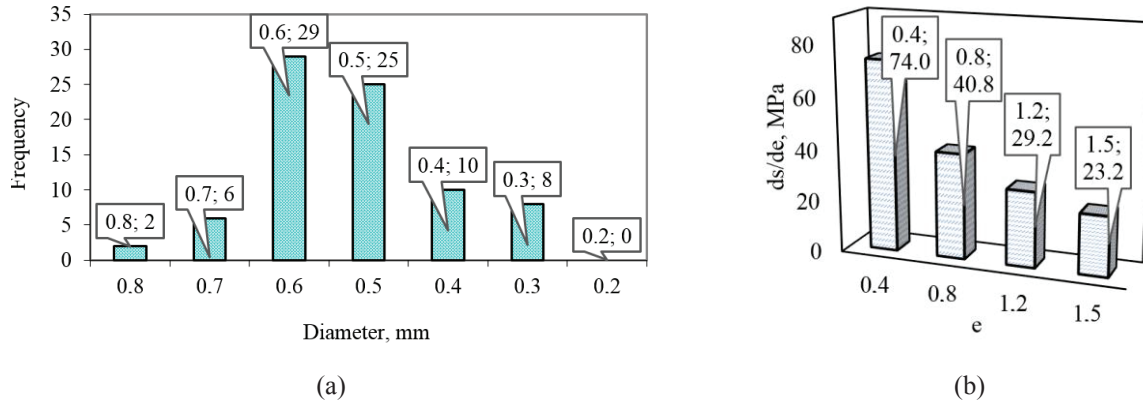


FIGURE 1. Breakage frequency distribution in the drawing route (a) and the flow stress derivative with respect to the amount of strain in the drawing passes (b)

Figure 1 (b) shows that the differential value is reduced in the drawing route, and this is indicative of a decrease in the intensity of hardening. Then the stress-strain state in the first drawing pass is calculated and strain distribution in the workpiece volume is determined. The workpiece with inherited uneven deformation is "transferred" to the next calculation stage with another drawing tool geometry, typical of the second drawing pass, and calculations are made again, and so on.

For specific strain rate tensor components ξ_{ij} , the strain state is described by shear strain rate intensity H , strain rate ξ and the amount of shear strain, they being determined, respectively, as

$$H = \sqrt{2\xi_{ij}\xi_{ij}}; \quad (4)$$

$$\xi = H/\sqrt{3}; \quad (5)$$

$$\Lambda = \int_0^t H d\tau, \quad (6)$$

where t is the deformation time.

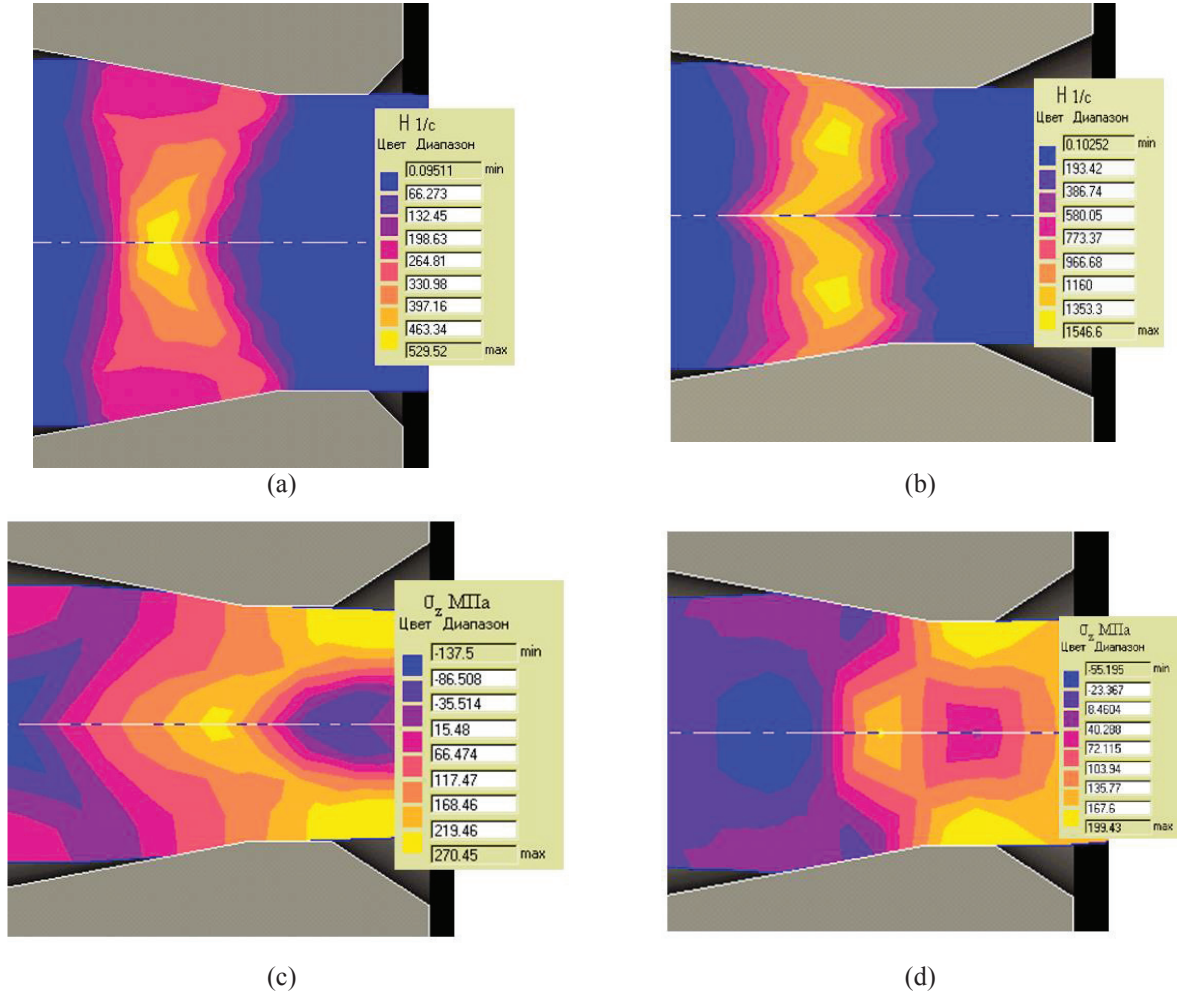


FIGURE 2. Shear strain rate intensity H for the first (a) and fourth (d) passes and stress σ_{zz} for the first (c) and fourth (d) passes of wire drawing

The calculated friction coefficient equals to 0.1. Not only power-law hardening, but also strain-rate one is taken into account in the solution of the problem. It is assumed that the drawing is performed in a multipass machine, with the volume-second constancy; therefore, the linear velocity increases in proportion to the extension ratios. At the entrance to the first die of the route, the linear velocity is 1.3 m/s.

The shear strain rate intensity H for the first and fourth passes of wire drawing is presented in fig. 2, a, b. The stress σ_{zz} for the first and fourth passes are shown in fig. 2, c, d. In the first pass there is only one zone of high strain rates (fig. 2, a).

There are visible differences caused by the reduction of the derivative $d\sigma_s/d\varepsilon$ from 74.0 to 23.2 MPa; namely, the particle motion path in the workpiece center has extended and there have appeared two strain rate intensity peaks instead of one, and their location corresponds to the relative radial coordinate 0.6 ... 0.8. It was noted

in [8] that, at the same coordinate, the highest angle of the misorientation of the texture component $\{111\}$ is observed. In addition, in the deformation zone there is a zone of increased axial tensile stress σ_{zz} (fig. 2, c, d) that provokes rupture. The division of the deformation zone into two parts about the workpiece axis in the first and fourth passes (fig. 2, b) creates a risk of macropores and breakage localization, which is shown experimentally in the first part of the paper.

CONCLUSION

Industrial data on the frequency of breakage in copper wire drawing have been presented. Special attention is paid to the fact that the maximum breakage frequency does not coincide with the maximum amount of strain accumulated in the wire. A hypothesis about the effect of metal texture, which changes in the drawing route with the intensity of metal hardening, on metal breakage has been proposed. A finite element solution to the boundary value problem of wire drawing has been discussed.

ACKNOWLEDGMENTS

This work was done within the state order on subject No. 01201375904 and supported by RF Government decree No. 211, contract No. 02.A03.21.0006.

REFERENCES

1. Yu. N. Loginov, S. L. Demakov, M. A. Ivanova, A. G. Illarionov, M. S. Karabanalov, S. I. Stepatov, *Physics of Metals and Metallography* **116** (4), 393–400 (2015).
2. Masafumi Matsushita, Tomoya Kuji, Hiromitsu Kuroda, Seigi Aoyama, Hiroaki Ohfuji, *Materials Sciences and Application* **2**, 911–916 (2011).
3. Krishna Rajan, Ronald Petkie, *Materials Science and Engineering* **257**, 185–197 (1998).
4. Pal-Val, P. P., Natsik, V. D., Pal-Val, L. N., Loginov, Yu. N., Demakov, S. L., Illarionov, A. G., Davydenko, A. A., Rybalko, A. P., *Materials Science and Engineering* **618**, 9–15 (2014).
5. S. L. Demakov, Yu. N. Loginov, A. G. Illarionov, M. A. Ivanova, M. S. Karabanalov, *Physics of Metals and Metallography* **113** (7), 681–686 (2012).
6. A. Bhattacharyya, D. Rittel, G. Ravichandran, *Scripta Materialia*, **52**, 657–661 (2005).
7. Yu. N. Loginov, S. L. Demakov, A. G. Illarionov, M. A. Ivanova, *Russian Metallurgy (Metally)* **11**, 947–952 (2012).
8. Yu. N. Loginov, S. L. Demakov, A. G. Illarionov, A. A. Popov, *Russian metallurgy (Metally)* **3**, 194–201 (2011).